ELSEVIER

Theoretical and Applied Fracture Mechanics 27 91997) 213–220

theoretical and applied fracture mechanics

Residual strength of a fiber reinforced metal matrix composite with a crack

Z.H. Jin, R.C. Batra *

Department of Engineering Science and Mechanics, Virginia Polytechnic Institute and State University, Blacksburg, VA 24061-0219, USA

Abstract

The residual strength of a cracked unidirectional fiber reinforced metal matrix composite is studied. We propose a bridging model based on the Dugdale strip yielding zones in the matrix ahead of the crack tips that accounts for ductile deformations of the matrix and fiber debonding and pull-out in the strip yielding zone. The bridging model is used to study the fracture of an anisotropic material and its residual strength is calculated numerically. The predicted results for a SiC/titanium composite agree well with the existing experimental data. It is found that a higher fiber bridging stress and a larger fiber pull-out length significantly contribute to the composite's residual strength. The composite's strength may be more notch-insensitive than the corresponding matrix material's strength depending on several factors such as fiber–matrix interface properties and the ratio of the matrix modulus to an 'effective modulus' of the composite. © 1997 Elsevier Science B.V.

1. Introduction

The interest in fiber reinforced metal matrix composites (MMC's) is still growing because of their advantages including high toughness, and resistance to impact and thermal shock over ceramic matrix composites (CMC's) and polymer matrix composites (PMC's). Even though substantial progress has been made in understanding the strength of MMC's [1–10], satisfactory theoretical predictions of their strength in the presence of notches and cracks can not be made. However, this is essential for the design of aerospace and other engineering components. The notch strength behavior of MMC's is different from that of their matrices. There should also be significant differences between the notch strength behaviors of MMC's and CMC's since the metal matrices in MMC's are much more ductile than the ceramic matrices in CMC's. Connell et al. [10] used a crack-bridging concept to predict the notch strength of a unidirectional SiC fiber reinforced titanium alloy. Though their predicted strength agreed well with the measured values, their model does not consider micromechanical processes such as fiber debonding, frictional slip and pull-out and the bridging stress was estimated from the tensile test data. Furthermore, they assumed that bridging was lost in the wake of the matrix crack. However, the broken fibers, in the pull-out process, may still bridge the matrix crack [11].

We propose here a model, based on the Dugdale strip yielding and micromechanical analyses of fiber debonding and pull-out and use a singular integral equation method to predict the residual strength of a unidirectionally fiber reinforced MMC with a through

* Corresponding author. Fax: +1-540-2314574; e-mail: rbatra@vt.edu.

0167-8442/97/$17.00
PII S0167-8442(97)00023-2

crack. The effects of bridging stress and fiber pull-out length on the residual strength are studied. The predicted strength of a unidirectionally SiC fiber reinforced titanium matrix composite with a central crack is found to agree well with the experimental data.

2. Governing equations

We consider plane stress elastic deformations of a unidirectionally fiber-reinforced metal matrix plate. Assuming that it can be regarded as orthotropic, equations governing its deformations are [12]

$$\begin{aligned}\beta_1\frac{\partial^2 v_1}{\partial y_1^2}+\frac{\partial^2 v_1}{\partial y_2^2}+\beta_2\frac{\partial^2 v_2}{\partial y_1\partial y_2}=0,\\ \frac{\partial^2 v_2}{\partial y_1^2}+\beta_1\frac{\partial^2 v_2}{\partial y_2^2}+\beta_2\frac{\partial^2 v_1}{\partial y_1\partial y_2}=0,\end{aligned}\tag{1}$$

where the transformed stresses $\tau_{\alpha\beta}$ (subscripts α and β take values 1 and 2) and stresses $\sigma_{\alpha\beta}$ are related to the transformed displacements v_α by

$$\begin{aligned}\tau_{11}&=\frac{\sigma_{11}}{\lambda}=\frac{E_0}{1-\nu_0^2}\left(\frac{\partial v_1}{\partial y_1}+\nu_0\frac{\partial v_2}{\partial y_2}\right),\\ \tau_{22}&=\lambda\sigma_{22}=\frac{E_0}{1-\nu_0^2}\left(\frac{\partial v_2}{\partial y_2}+\nu_0\frac{\partial v_1}{\partial y_1}\right),\\ \tau_{12}&=\sigma_{12}=\frac{E_0}{2(\kappa+\nu_0)}\left(\frac{\partial v_1}{\partial y_2}+\frac{\partial v_2}{\partial y_1}\right).\end{aligned}\tag{2}$$

In Eqs. (1) and (2), the transformed coordinates y_α and the transformed displacements v_α are given by

$$y_1=x_1/\sqrt{\lambda},\qquad y_2=x_2\sqrt{\lambda},\tag{3}$$

$$v_1=u_1\sqrt{\lambda},\qquad v_2=u_2/\sqrt{\lambda},\tag{4}$$

where x_α are rectangular Cartesian coordinates and u_α the displacements of a point. Various constants in Eqs. (1)–(4) are given by [12,13]

$$\begin{aligned}\beta_1&=2(\kappa+\nu_0)/(1-\nu_0^2),\\ \beta_2&=\nu_0\beta_1+1,\end{aligned}\tag{5}$$

$$\begin{aligned}E_0&=\sqrt{E_{11}E_{22}},\qquad \nu_0=\sqrt{\nu_{12}\nu_{21}},\\ \lambda&=(E_{11}/E_{22})^{1/4},\qquad \kappa=E_0/(2\mu_{12})-\nu_0,\end{aligned}\tag{6}$$

where E_{11}, E_{22}, μ_{12}, ν_{12} and ν_{21} are elastic constants of the orthotropic plate. For a unidirectionally reinforced MMC with fibers in the x_1-direction [14–16],

$$\begin{aligned}E_{11}&=V_fE_f+(1-V_f)E_m,\\ E_{22}&=\frac{1+2\eta V_f}{1-\eta V_f}E_m,\quad \eta=\frac{E_f/E_m-1}{E_f/E_m+2},\\ \mu_{12}&=\frac{(1+V_f)\mu_f+(1-V_f)\mu_m}{(1-V_f)\mu_f+(1+V_f)\mu_m}\mu_m,\\ \nu_{12}&=\frac{E_{11}}{E_{22}}\nu_{21}=V_f\nu_f+(1-V_f)\nu_m,\end{aligned}\tag{7}$$

where V_f is the fiber volume fraction and subscripts f and m stand for the fiber and the matrix, respectively.

3. The proposed model and the problem formulation

Consider an infinite unidirectionally fiber reinforced MMC plate with a through crack of length $2a_0$ perpendicular to the fiber direction. The plate is subjected to a uniform tension σ_∞ at infinity in the fiber (x_1)-direction.

For a SiC fiber reinforced titanium alloy (Ti–6Al–4V), Connell et al. [10] observed a narrow plastic strip ahead of the crack tip and essentially all fibers within the plastic zone broke prior to the catastrophic fracture of the plate. Based on the experimental observations, they proposed a two level rectilinear bridging law, i.e. the plastic strip is treated as a bridged crack and the crack bridging stress is governed by the unnotched composite's strength during the first stage and by the matrix yield stress with a contribution from fiber pull-out during the second stage following fiber breakage. The bridging is lost when the local strain reaches the failure strain of the matrix. This model does not consider fiber debonding, frictional slip and pull-out processes which will definitely influence the bridging law, a relationship between the bridging stress and the separation of the bridged crack faces. Also, fiber bridging is not necessarily lost in the wake of the matrix crack as the

broken fibers in the pull-out process may still bridge the matrix crack [11].

Here we propose a bridging model based on both matrix yielding and micromechanical analyses of fiber debonding and pull-out. It is assumed that both the matrix and fibers contribute to the bridging stress, i.e.

$$\sigma = V_m \sigma_m + V_f \sigma_f \tag{8}$$

where $V_m = 1 - V_f$, σ is the total bridging stress, σ_m the stress due to matrix yielding and σ_f the stress due to fiber debonding and pull-out. It is reasonable to assume that σ_m is given by the Dugdale model [17]

$$\sigma_m = \sigma_s H(\delta_s - \delta) \tag{9}$$

where δ is the separation between the upper and lower surfaces of the yielding zone (faces of the bridged crack), σ_s is the yield stress of the matrix, δ_s is the critical separation at which crack growth occurs in the matrix and $H(\cdot)$ is the Heaviside step function. δ_s is related to the yield stress and the critical value, J_c, of the J-integral by

$$\delta_s = J_c/\sigma_s. \tag{10}$$

The bridging stress σ_f due to fibers can be determined from micromechanics analyses of the stress transfer between fibers and matrix [18], fiber debonding [19–21] and fiber pull-out. As we replace the strip yielding zone by a bridged crack, the elastic analyses [18–20] may be validated in the elastic region at the bridged crack face and approximately apply to the debonding bridging in the real problem. The elastic analyses [19–21] have also been employed to study the fatigue crack growth [22,23]. In the first stage fibers are intact and are bonded perfectly to the matrix. When the shear stress at the interface between the fiber and the matrix reaches a critical value, the fiber is debonded from the matrix but still remains unbroken. Usually, the energy contribution from the first stage is negligibly small and we will not consider bridging during this stage. In fact, we will see below that the bridging energy of fiber debonding and slipping is also very small as compared with the fiber pull-out energy in MMC's especially when the fiber-matrix interface is not too weak. In the debonding stage, σ_f is related to the separation δ by [20,21]

$$\sigma_f/\sigma_0 = \sqrt{\delta/\delta_0}\, H(\delta_0 - \delta) \tag{11}$$

where σ_0 is the fiber strength (here we assume that fibers have a deterministic strength),

$$\delta_0 = \frac{(1 - V_f)^3 E_m^2 \sigma_0^2}{2\tau E_f E_{11}^2} R, \tag{12}$$

R is the fiber radius and τ the frictional shear stress at the interface between the fiber and the matrix. When the fiber stress reaches the fiber strength σ_0, fibers are broken and are subsequently pulled out. The pull-out stress may be obtained through a simple shear lag analysis.

$$\sigma_f/\sigma_c = [1 - (\delta - \delta_0)/(\delta_c - \delta_0)] \times H(\delta_c - \delta) H(\delta - \delta_0) \tag{13}$$

where δ_c is the fiber pull-out length and σ_c a critical stress. Usually σ_c is less than σ_0. It is expected that the stress in the fiber drops rather precipitously from σ_0 to σ_c immediately after it breaks. The stress drop $\sigma_0 - \sigma_c$ is a characteristic of the fiber–matrix interface properties. A simple shear lag analysis gives

$$\sigma_c = \frac{2\tau\delta_c}{R}. \tag{14}$$

δ_c in Eqs. (13) and (14) is not a constant but varies from fiber to fiber. Here we assume that there exists a statistical average value of δ_c determined experimentally and use it below. As mentioned above, for MMC's, the fiber debonding energy is generally negligibly small as compared with the fiber pull-out energy and $\delta_0 \ll \delta_c$. For example, for a SiC/titanium composite studied in [6,10], $\delta_0 = 0.1$ μm, the debonding energy $G_d = 0.032$ kJ/m^2, the average fiber pull-out length exceeds 100 μm and the pull-out energy is a fraction of the bridging energy, 72 kJ/m^2. Hence, the contribution from fiber debonding may be ignored in the residual strength calculations. However, it is more reasonable to regard the debonding energy as the crack tip energy because the scale of this debonding bridging is usually very small as compared with other bridging scales and macro-crack lengths. The debonding bridging scale may be characterized by the parameter $\bar{E}_0 \delta_0/(V_f \sigma_0)$ [24], where $\bar{E}_0$ is an 'effective modu-

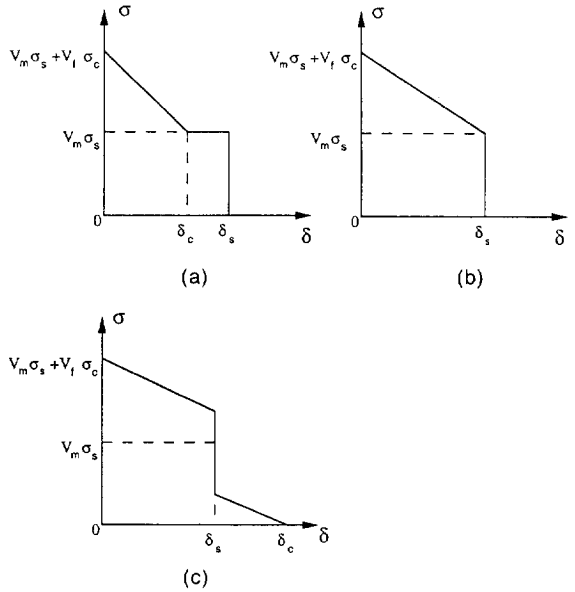

Fig. 1. Schematic representation of bridging curves, (a) $\delta_c < \delta_s$, (b) $\delta_c = \delta_s$ and (c) $\delta_c > \delta_s$.

lus' of the cracked orthotropic plate given below. For the SiC/titanium composite [6], this parameter equals about 36 μm which is an order of magnitude smaller than the macro-crack length in MMC's. Hence, we assume that the bridging stress due to fibers is fully described by Eq. (13) with $\delta_0 = 0$ and a crack tip energy $G_c = G_d$ exists. A schematic representation of the bridging law described by Eqs. (8), (9) and (13) is shown in Fig. 1.

Based on the above assumptions, the boundary conditions of the problem can be expressed as

$$\sigma_{11} = -\sigma_\infty + H(|x_2| - a_y)(1 - V_f)\sigma_s + H(|x_2| - a_d)V_f\sigma_c(1 - \delta/\delta_c), \quad x_1 = 0,\ |x_2| \le a, \tag{15}$$

$$\sigma_{12} = 0, \quad x_1 = 0, \quad |x_2| < \infty, \tag{16}$$

$$u_1 = 0, \quad x_1 = 0, \quad |x_2| > a, \tag{17}$$

where $a = a_0 + \Delta a$ is half of the length of the initial crack plus the length of the yielding/bridging zone, a_d and a_y initially equal a_0 and become larger when complete fiber pull-out and/or real crack growth in the matrix occur.

The boundary value problem defined by Eqs. (1), (2), (15)–(17) with transformed variables (Eqs. (3) and (4)) results in the following singular integral equation:

$$\frac{1}{2\pi}\int_{-1}^{1}\frac{\phi(s)\,ds}{s-r} + H(|r| - r_d)V_f\left(\frac{a}{a_0}\right) \times 2a_0^*\frac{\sigma_c/\sigma_s}{\delta_c/\delta_s}\int_{-1}^{r}\phi(s)\,ds = -\frac{\sigma_\infty}{\bar{E}_0} + H(|r| - r_y)(1 - V_f)\frac{\sigma_s}{\bar{E}_0} + H(|r| - r_d)V_f\frac{\sigma_c}{\bar{E}_0}, \quad |r| \le 1, \tag{18}$$

where

$$\phi(r) = \frac{\partial u_1(0, x_2)}{\partial x_2} \tag{19}$$

is the dislocation density along the crack (including the bridged part) face, $r = x_2/a$, $r_d = a_d/a$, $r_y = a_y/a$,

$$\bar{E}_0 = \frac{2\lambda E_0}{\sqrt{2(1+\kappa)}} \tag{20}$$

is an 'effective Young's modulus' of the orthotropic material, i.e. the cracked orthotropic material behaves like an isotropic one with 'Young's modulus' $\bar{E}_0$ and

$$a_0^* = \frac{a_0}{\bar{E}_0\delta_s/\sigma_s} \tag{21}$$

is a nondimensional crack length. The separation displacement of the crack faces is related to ϕ by

$$\delta = 2u_1(0, x_2) = 2a\int_{-1}^{r}\phi(s)\,ds. \tag{22}$$

It is clear that ϕ satisfies

$$\int_{-1}^{1}\phi(s)\,ds = 0. \tag{23}$$

According to the singular integral equation method [25,26], Eq. (18) under the condition in Eq. (23) has a solution of the form

$$\phi(r) = \frac{\psi(r)}{\sqrt{1-r^2}}, \quad |r| < 1, \tag{24}$$

where $\psi(r)$ is continuous and bounded on $[-1, 1]$.

The stress intensity factor at the tip of the bridged crack can be evaluated from

$$K_{tip} = -\frac{1}{2}\bar{E}_0\sqrt{\pi a}\,\psi(1) \tag{25}$$

and the crack tip energy release rate is given by

$$G_{tip} = \frac{K_{tip}^2}{\bar{E}_0}. \tag{26}$$

4. Residual strength

For a given initial crack, Eq. (18) can be solved with increasing yielding/bridging length and the strength σ_∞ can be evaluated from Eqs. (24)–(26) with $G_{tip} = G_c$. For a monolithic metal panel, the residual strength is reached when the opening displacement at the initial crack tip or the tail of the yielding strip equals $\delta_c (= J_c/\sigma_s)$. For the MMC, the residual strength is determined by choosing the maximum value of the applied stress σ_∞ during the bridged crack growth.

It is convenient to write the solution of Eq. (18) as

$$\phi(r) = \frac{1}{\bar{E}_0}\left[\sigma_\infty\phi_1(r) + \sigma_s\phi_2(r) + \sigma_c\phi_3(r)\right] \tag{27}$$

where $\phi_i(r)$ $(i = 1, 2, 3)$ is dimensionless and satisfies

$$\frac{1}{2\pi}\int_{-1}^{1}\frac{\phi_i(s)\,ds}{s-r} + H(|r| - r_d)V_f\left(\frac{a}{a_0}\right)2a_0^*\frac{\sigma_c/\sigma_s}{\delta_c/\sigma_s}\int_{-1}^{r}\phi_i(s)\,ds = L_i(r), \quad |r| \le 1, \tag{28}$$

and

$$\int_{-1}^{1}\phi_i(s)\,ds = 0, \tag{29}$$

where

$$L_1(r) = -1, \qquad L_2(r) = H(|r| - r_y)(1 - V_f), \qquad L_3(r) = H(|r| - r_d)V_f. \tag{30}$$

Eq. (28) has a solution of the form

$$\phi_i(r) = \frac{\psi_i(r)}{\sqrt{1-r^2}}, \quad i = 1, 2, 3, \tag{31}$$

where $\psi_i(r)$ is continuous and bounded on $[-1, 1]$. The stress intensity factor at the tip of the bridged crack can then be evaluated from

$$K_{tip} = -\frac{1}{2}\sqrt{\pi a}\left[\sigma_\infty\psi_1(1) + \sigma_s\psi_2(1) + \sigma_c\psi_3(1)\right]. \tag{32}$$

By equating K_{tip} to the assumed critical effective stress intensity factor K_c and noting that

$$K_c = \sqrt{\bar{E}_0 G_c} \tag{33}$$

where G_c is the fiber debonding energy regarded as the crack tip energy, we obtain the following expression for the residual strength:

$$\frac{\sigma_R}{\sigma_s} = \max_{a \ge a_0}\left(\frac{1}{-(1/2)\psi_1(1)} \times\left\{\left[\frac{1 - V_f + (1/2)V_f(\sigma_c/\sigma_s)(\delta_c/\delta_s)}{\pi a_0^*}\frac{G_c}{G_b}\right]^{1/2} \times\frac{1}{\sqrt{a/a_0}} - \left[-\frac{1}{2}\psi_2(1)\right] - \frac{\sigma_c}{\sigma_s}\left[-\frac{1}{2}\psi_3(1)\right]\right\}\right) \tag{34}$$

Here

$$G_b = \sigma_s\delta_s\left[(1 - V_f) + \frac{1}{2}V_f\frac{\sigma_c}{\sigma_s}\frac{\delta_c}{\delta_s}\right] \tag{35}$$

is the bridging energy.

5. Numerical results and discussion

We first consider a SiC/titanium composite studied in Refs. [6,10]. By equating the bridging energy G_b in Eq. (35) to the experimental value 72 kJ/m^2 given in Ref. [10] and using the material properties data given in Ref. [6], we obtain $\sigma_c/\sigma_s = 0.754$, $\delta_c/\delta_s = 1.8125$ and $\bar{E}_0\delta_s/\sigma_s = 14.5$ mm. The calculated residual strengths for half crack lengths $a_0 =$ 0.75, 1.5 and 3.0 mm are 894, 870 and 807 MPa, respectively, which are close to the experimental values [10] of 910, 850 and 810 MPa, respectively. The effects of the specimen size and strain hardening of the matrix are not considered. A finite specimen

will have lower residual strength than an infinite one, and strain hardening tends to increase the strength. Thermal residual stress effects are also not included in the present model. Though the effect is significant in determining the overall tensile behavior of MMC's [27,28], it may not strongly influence the residual strength of cracked MMC's.

Figs. 2–4 show the calculated normalized residual strength $\sigma_R^* = \sigma_R/\sigma_s$ versus the nondimensional crack length $a_0^* = a_0/(\bar{E}_0\,\delta_s/\sigma_s)$ for various values of the bridging to yielding stress ratio σ_c/σ_s and the critical displacement ratio δ_c/δ_s. The effective crack tip energy is neglected in the calculations since it is much smaller than the bridging energy as shown in Section 3. It can be seen from Figs. 2–4 that for fixed δ_c/δ_s the residual strength increases with an increase in σ_c/σ_s. However, the material becomes more notch-sensitive for larger values of σ_c/σ_s, i.e. for large σ_c/σ_s, the residual strength decreases more rapidly with an increase in the initial crack length, especially for short cracks. For fixed σ_c/σ_s, the residual strength increases with an increase in δ_c/δ_s and the composite's strength becomes less notch-sensitive. Fig. 5 shows the residual strength for a composite and for the corresponding metal matrix

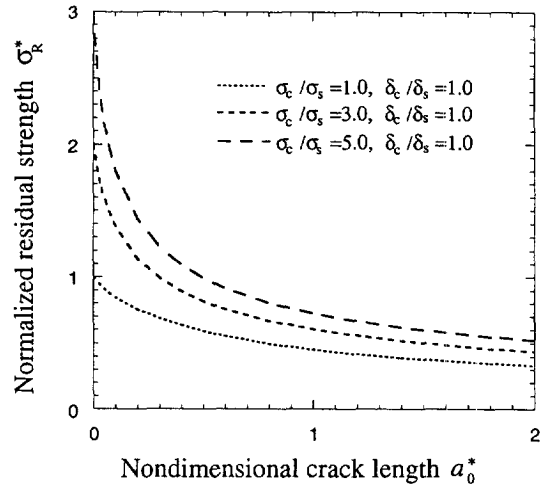

Fig. 3. Normalized residual strength versus nondimensional crack length for various bridging to yielding stress ratios and δ_c/δ_s = 1.0.

with $\bar{E}_0/E_m = 2.0$. The metal's residual strength is obtained from the Dugdale model

$$\frac{\sigma_R}{\sigma_s} = \frac{2}{\pi}\cos^{-1}\left(e^{-\left(\frac{E_m}{\bar{E}_0}\frac{\pi}{8a_0^*}\right)}\right). \tag{36}$$

We note that, for this case, the metal's strength is more notch-sensitive than the composite's except for very short cracks. However, the composite may be-

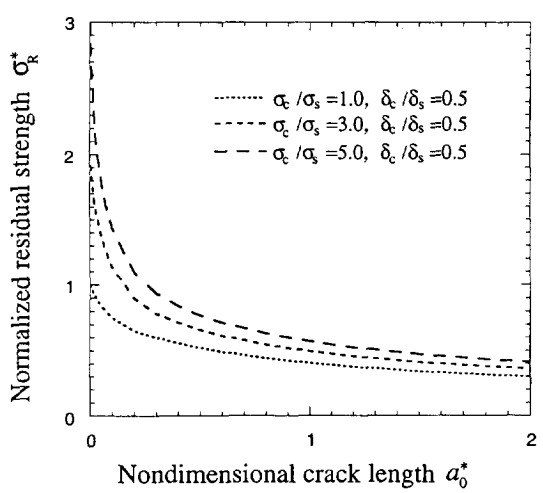

Fig. 2. Normalized residual strength versus nondimensional crack length for various bridging to yielding stress ratios and δ_c/δ_s = 0.5.

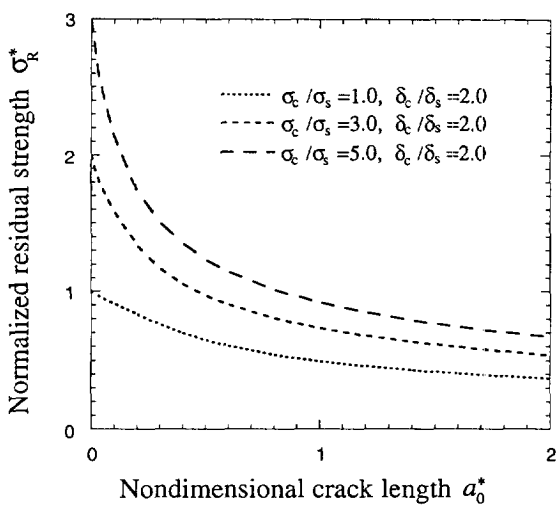

Fig. 4. Normalized residual strength versus nondimensional crack length for various bridging to yielding stress ratios and δ_c/δ_s = 2.0.

come more notch-sensitive than the matrix for lower values of δ_c/δ_s and $\bar{E}_0/E_m$. Hence, improved damage tolerance of MMC's may be achieved by increasing δ_c/δ_s and $\bar{E}_0/E_m$. A higher δ_c/δ_s may be promoted by a weak fiber–matrix interface so that fibers break randomly in the plastic region giving a higher average pull-out length. However, a very weak interface will lower the fiber bridging stress resulting in a low residual strength of the composite. Hence, the fiber-matrix interface has to be optimized. We note that we have assumed a deterministic fiber strength. A statistical consideration of the fiber strength may result in a scattered residual strength distribution with a statistical average approximately described by the proposed model.

The model developed here for fiber reinforced MMC's may also be applied to particulate MMC's. For particulate MMC's, the critical displacement ratio δ_c/δ_s is low as δ_c now represents the average particle size. The stress ratio σ_c/σ_s is also low as σ_c is proportional to δ_c. Also, particle rupture often occurs in particulate MMC's. Hence, the particle bridging effect will not be significant. Fig. 6 shows the residual strength of a cracked particulate MMC. It is clear that particle bridging does not contribute much to the residual strength for cracks longer than $0.2E_0\delta_s/\sigma_s$ (E_0 is the effective modulus of the particulate MMC).

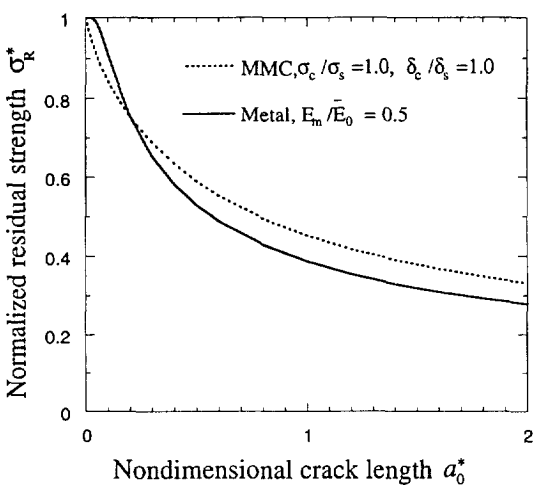

Fig. 5. Normalized residual strength versus nondimensional crack length for a fiber MMC ($\sigma_c/\sigma_s = 1.0$ and $\delta_c/\delta_s = 1.0$) and that for the corresponding metal matrix.

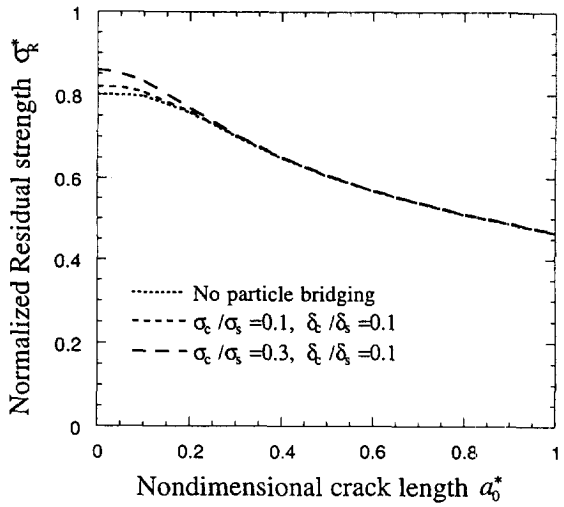

Fig. 6. Normalized residual strength versus nondimensional crack length for a particulate MMC.

6. Concluding remarks

The crack bridging concept is used to study the residual strength of a cracked unidirectionally fiber-reinforced metal matrix composite. Dugdale strip yielding in the matrix and effects of fiber debonding and pull-out from the matrix are included in the analysis. The anisotropy of the material is considered through an effective modulus. The predicted results for a SiC/titanium composite agree well with the existing experimental data. It is found that a higher fiber bridging stress and a larger fiber pull-out length significantly contribute to the composite's residual strength. The notch sensitivity of the composite's strength depends upon several factors such as the fiber–matrix interface properties and the ratio of the matrix modulus to an 'effective modulus' of the composite.

References

[1] K.G. Kreider (Ed.), Metallic Matrix Composites, Academic Press, New York, 1974.

[2] S. Suresh, A. Mortensen, A. Needleman (Eds.), Fundamentals of Metal Matrix Composites, Butterworth-Heinemann, Boston, 1993.

[3] S. Jansson, H.E. Deve, A.G. Evans, The anisotropic mechanical properties of Ti matrix composite reinforced with SiC fibers, Metall. Trans. 22A (1991) 2975–2984.
[4] S.L. Draper, P.K. Brindley, M.V. Nathal, Effect of fiber strength on the room temperature tensile properties of SiC/Ti–24Al–11Nb, Metall. Trans. 23A (1992) 2541–2548.
[5] W.A. Gurtin, Ultimate strengths of fiber-reinforced ceramics and metals, Composites 24 (1993) 98–102.
[6] C.H. Weber, X. Chen, S.J. Connell, F.W. Zok, On the tensile properties of a fiber reinforced titanium matrix composite. I. Unnotched behavior, Acta Metall. Mater. 42 (1994) 3443–3450.
[7] S.L. Draper, B.J. Aikin, J.J. Eldridge, Tensile behavior of Al_2O_3/FeAl+B and Al_2O_3/FeCrAlY composites, Metall. Trans. 26A (1995) 2719–2731.
[8] G.A. Bigelow, A micromechanics-based strength prediction methodology for notched metal matrix composites, Composites 24 (1993) 113–121.
[9] K.J. Venkateswara Rao, S.C. Siu, R.O. Ritchie, Failure mechanisms in SiC-fiber reinforced 6061 aluminum alloy composites under monotonic and cyclic loading, Metall. Trans. 24A (1993) 721–734.
[10] S.J. Connell, F.W. Zok, Z.Z. Du, Z. Suo, On the tensile properties of a fiber reinforced titanium matrix composite. II. Influence of notches and holes, Acta Metall. Mater. 42 (1994) 3451–3461.
[11] J.G. Bakuckas Jr., J. Awerbuch, T.-M. Tan, A.C.W. Lau, Evaluation of notch-tip damage in metal-matrix composites during static loading, in: R. Chona (Ed.), Fracture Mechanics, vol. 23, ASTM/STP 1189, American Society for Testing and Materials, Philadelphia, 1993, pp. 713–737.
[12] F. Erdogan, B. Wu, Interface crack problems in layered orthotropic materials, J. Mech. Phys. Solids 41 (1993) 889–917.
[13] S. Krenk, On the elastic constants of plane orthotropic elasticity, J. Composite Mater. 13 (1979) 108–116.
[14] R.M. Christensen, Mechanics of Composite Materials, Wiley, New York, 1979.
[15] S.W. Tsai, H.T. Hahn, Introduction to Composite Materials, Technomic Publishing, Westport, CT, 1980.
[16] Z.C. Xia, R.R. Carr, J.W. Hutchinson, Transverse cracking in fiber-reinforced brittle matrix, cross-ply laminates, Acta Metall. Mater. 41 (1993) 2365–2376.
[17] D.S. Dugdale, Yielding of steel sheets containing slits, J. Mech. Phys. Solids 8 (1960) 100–104.
[18] L.N. McCartney, New theoretical model of stress transfer between fiber and matrix in a unidirectionally fiber-reinforced composite, Proc. R. Soc. London A 425 (1989) 215–244.
[19] D.B. Marshall, B.N. Cox, A.G. Evans, The mechanics of matrix cracking in brittle matrix fiber composites, Acta Metall. 33 (1985) 2013–2021.
[20] L.N. McCartney, Mechanics of matrix cracking in brittle-matrix fiber reinforced composites, Proc. R. Soc. London A 409 (1987) 429–450.
[21] J.W. Hutchinson, H.M. Jensen, Models of fiber debonding and pull-out in brittle composites with friction, Mech. Mater. 9 (1990) 139–163.
[22] R.M. McMeeking, A.G. Evans, Matrix fatigue cracking in fiber composites, Mech. Mater. 9 (1990) 217–227.
[23] G. Bao, R.M. McMeeking, Fatigue crack growth in fiber-reinforced metal–matrix composites, Acta Metall. Mater. 42 (1994) 2415–2425.
[24] G. Bao, Z. Suo, Remarks on crack bridging concepts, Appl. Mech. Rev. 45 (1992) 355–366.
[25] N.I. Muskhelishvili, Singular Integral Equations, Noordhoff, Groningen, 1953.
[26] F. Erdogan, G.D. Gupta, T.S. Cook, Numerical solution of singular integral equations, in: G.C. Sih (Ed.), Mechanics of Fracture, vol. 1, Noordhoff, Leyden, 1973, pp. 368–425.
[27] R.J. Arsenault, Strengthening of metal matrix composites due to dislocation generation through CTE mismatch, in: R.K. Everett, R.J. Arsenault (Eds.), Metal Matrix Composites: Mechanism and Properties, Academic Press, Boston, 1991, pp. 79–100.
[28] T. Nakamura, S. Suresh, Effects of thermal residual stress and fiber packing on deformation of metal matrix composites, Acta Metall. Mater. 41 (1993) 1665–1681.